*Transactions of the Materials Research Society of Japan* 29[6] 2911-2914 (2004)

# Preparation of Hydroxyapatite/Chondroitin Sulfate Nanocomposite and its Spherical Porous Microparticle

Toshiyuki Ikoma*, ***, Norifumi Azuma** and Junzo Tanaka*, ***
*National Institute for Materials Science, Biomaterials Center and Namiki 1-1, Tsukuba, Ibaraki, Japan
Fax: 81-29-851-8291, e-mail: IKOMA.Toshiyuki@nims.go.jp, TANAKA.Junzo@nims.go.jp
** Biomaterial Laboratory, Faculty of Engineering, Okayama University and Tsushima, Okayama, Japan
Fax: 81-29-851-8291, e-mail: AZUMA.Norifumi@nims.go.jp
*** CREST, Japan Science and Technology Agency and Honcho 4-1-8, Kawaguchi, Saitama, Japan

Nanocomposites of hydroxyapatite (HAp)/chondroitin sulfate (ChS) with a spindle-shaped morphology of 150 × 50 nm in size were obtained using a self-organization, to enhance the initial calcium binding to the ChS. In the nanocomposites, the *c*-axis of HAp nanocrystals was oriented along the longitudinal axis of aggregations as the results of TEM, HRTEM. ChS in a suspension inhibited HAp crystal growth; the size of plate shaped crystals was decreased from 21 × 8.6 nm to 14 × 5.8 nm with the increase of ChS concentrations. Perfectly spherical porous microparticles by using a spray drying method were successfully developed with the size range of 1.0 to 20 μm, specific surface area of c.a. 100 $m^2g^{-1}$ and porosities of over 60 vol%. The spherical microparticles obtained had the compositions of 1 to 50 wt% of ChS against HAp with low crystallinity. No decomposition of ChS molecular chains was observed after the spray drying processes. It is worthy to note that the zeta-potential of spherical microparticles was gradually changed to be negative value of -28mV against 3.5mV of HAp microparticle. The spherical microparticles obtained are applicable to create more complicated composites and drug carriers.

Key words: Hydroxyapatite, Chondroitin Sulfate, Spray drying, Microparticle, Self-organization

## 1. INTRODUCTION

Chondroitin sulfate (ChS) is a kind of glycosaminoglycans (GAGs), which is the most abundant polysaccharide in the connective tissue of bone and cartilage [1]. The GAGs form spatial arms in proteoglycans (PGs) that play essential roles in tissue differentiation, cell migration and adhesion, and the regulation of mineralization [2]. The PGs of large sizes inhibit the formation and growth of hydroxyapatite (HAp) crystals by steric hindrance [3]. On the other hand, the reduction of calcium content in a solution containing highly anionic PGs has been reported to show calcium chelation. An activity of GAGs of a calcium chelation acts as mineralization promoters [4]. The ChS-containing decorin of bone binds to the surfaces of type I collagen fibrils, which regulates collagen fibrillogenseis by binding to fibronectin, heparin and growth factors [5]. The PGs of small sizes have a binding affinity for HAp crystals in the mineralized tissues and play an important role in mineralization [6].

There are many advantages to control the morphology and particle size of HAp ceramics [7]. The smaller particle sizes have the higher specific surface area and the higher bonding capacity of biopolymers and drugs. The spherical morphology has a benefit to prepare the inorganic/organic composites [8].

P. Luo and T.G. Nieh [7] fabricated the HAp granules with the size range of 1-8μm using a spray drying method. Commercially available spherical particles of HAp are typically 20-80 μm with a spray drying method. Porous HAp granules with the size range 0.3-4 mm were prepared by vibration and rolling of the synthetic HAp powders with water [9] and dripping a HAp solution into liquid nitrogen, drying and sintering [10] and a drip-casting process[11]. The perfectly spherical HAp granules with 125-1000 μm were prepared using solid-in-water-in-oil system (S/W/O emulsion) and then sintered [12].

HAp ceramics loaded with therapeutic agents have been developed for the delivery system and the time controlled release [13]. The specific surface area and particle sizes are of importance for the drug loading and release properties [14].

In the present study, we prepared HAp/ChS nanocomposites by mixing $Ca(OH)_2$ and ChS suspensions into a $H_3PO_4$ solution to enhance the initial calcium binding to the ChS, and to elucidate an inhibition of HAp crystal growth. Moreover, perfectly spherical microparticles were fabricated by using a spray drying method and the morphologies, particle size distributions and zeta potentials were analyzed to elucidate the powder properties.

## 2. EXPERIMENTAL

### 2.1 Preparation of HAp/ChS nanocomposite

The following synthesis method was used to ensure the purity of HAp and enhance the initial calcium binding to ChS to form the self-organized nanocomposites. Pure $CaCO_3$ powder was heated at 1050°C for 3 hours, and the resultant CaO powder was hydrated with distilled water to produce $Ca(OH)_2$. 1000 ml of 0.15 mol/l $H_3PO_4$ solution were dropped into 1000 ml of 0.25 mol/l $Ca(OH)_2$ suspension without or with sodium ChS (Seikagaku kougyo Co. Tokyo, Japan; the molecular weight of 15K with the 6-ChS/4-ChS ratio of 55/45) at room temperature by vigorous stirring. The dropping rate was controlled to 20 ml/min. The concentrations of ChS to mix into the $Ca(OH)_2$ suspension were 0.5, 1.25, 2.5, 5.0 and 12.5 mg/ml. The theoretical weight ratios of ChS/HAp were 2.0, 5,0, 10, 20 and 50wt%, respectively. The suspensions obtained were aged overnight; the final pH was adjusted to 8.0.

### 2.2 Preparation of spherical microparticle

Perfectly spherical porous microparticles of HAp/ChS nanocomposites were fabricated by a spray drying method: the suspensions of HAp/ChS nanocomposite were atomized under a pressure of 1.5 MPa at a flow rate of 500 ml/h, and inlet and outlet temperatures of a nozzle were adjusted to 150 and 60°C, respectively.

### 2.3 Characterization

The structures of the HAp/ChS nanocomposites were observed by transmission electron microscopy (TEM) and electron diffraction under an acceleration voltage of 200 KV, and the suspensions were mixed into ethyl alcohol, and dried. The porous microparticles of HAp/ChS nano-composites were employed for powder X-ray diffractometry (XRD), diffuse refractant Fourier transform infrared (FTIR) spectroscopy and thermogravimetry (TG-DTA) to elucidate the change of crystallite sizes, the incorporation of carbonate ions into HAp and the content of ChS in the microparticles. The crystallite sizes of HAp were estimated with the Sherrer's equation: the Sherrer's constant was calculated as 0.94.

The morphology of the microparticles was observed with scanning electron microscopy (SEM) with the acceleration voltage of 20KV after coated with platinum. The specific surface areas and total volumes were determined by Brunauer-Emmett-Teller method. The particle size distributions were analyzed by particle size analyzer of laser diffraction method. The samples were dispersed into distilled water. The zeta-potential was measured by DELSA515. The samples were dispersed into 0.01mol/l of $KNO_3$ electrolyte solutions with the weight ratio of 2mg/40ml.

## 3. RESULTS

Figure 1 shows the TEM images of the HAp/ChS nanocomposites obtained under various concentrations of ChS. The crystal sizes of the HAp in the nanocomposites were ca. 20 nm in length and 5 nm in width. At the concentrations lower than 2.5 mg/ml, the spindle-shaped aggregations of 150 nm in length and 50 nm in width were observed as shown in (a), and (b). It is worthy to note that the longitudinal length 150 nm is in good agreement with the length of the ChS molecule. The morphology of constituent nanocrystals was also a thin plate-like shape. As seen in the electron diffraction pattern, the diffractions of 002 and 004 formed clear spots along the longitudinal axis of the corresponding spindle-shaped aggregation; therefore, the *c*-axes of the constituent HAp nanocrystals were aligned parallel with the longitudinal axis of the aggregation.

At the concentrations higher than 5.0 mg/ml, the spindle-shaped aggregations were not observed. This indicated that the repulsion among ChS molecules inhibited the formation of spindle-shaped aggregations.

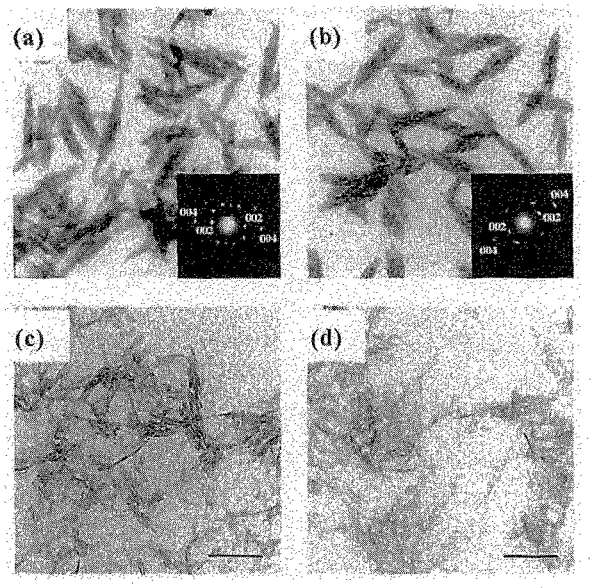


Fig. 1 TEM images of HAp/ChS nano- composites prepared at various ChS concentrations; (a) 0.5mg/ml, (b) 2.5 mg/ml, (c) 5.0 mg/ml and (d) 12.5 mg/ml. The bar is 100 nm.

XRD patterns of the microparticles showed that the calcium phosphate obtained was a single phase of HAp with low crystallite. The widths of diffraction profiles clearly decreased with the increase of the concentration of ChS.

Figure 2 shows the change of crystallite sizes along *a*- and *c*-axis calculated from 002 and 200 diffractions of HAp. Both crystallite sizes obviously decreased against the concentration of ChS. The HAp formation was not inhibited at 0.5 mg/ml of ChS, and the inhibition of HAp crystal growth was clearly observed at over 2.5 mg/ml. The maximum inhibition of HAp crystal growth occurred at 25 mg/ml of ChS, and the inhibition rate was almost 32%. The present results matched with the reported data [2,3].

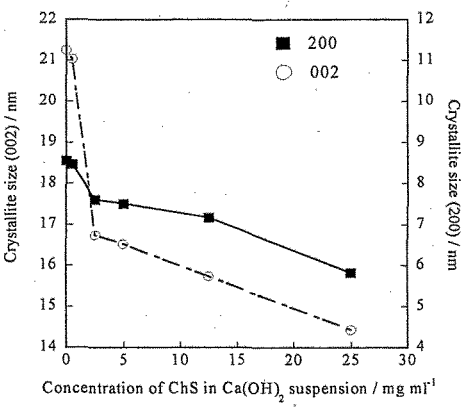


Fig. 2 Change of the crystallite sizes of 002 and 200 diffractions against the concentration of ChS in $Ca(OH)_2$ suspension.

FTIR spectra of the HAp/ChS microparticles indicated that the stretching mode of the $PO_4$ group was detected at 1093, 1035, 967, 607 and 568 $cm^{-1}$ in all samples. Two stretching modes and an out-of-plane mode of the $CO_3$ group were at 1453, 1424 and 879 $cm^{-1}$ that indicated the $CO_3$ group partially substituted the $PO_4$ group. Thus, the HAp crystals obtained had the compositions similar to a biological apatite[7]. The asymmetric stretching modes of the $SO_3$ groups were observed at 1268 and 1229 $cm^{-1}$, which showed a red chemical shift compared with that of 1235 $cm^{-1}$ of the sodium ChS specimen. This suggests that the chemical interaction of the $SO_3$ group on the ChS chain with calcium ions could occur. The absorption bands of carboxyl groups could not be detected due to overlapping of the band of absorbed water at around 1613 $cm^{-1}$, however the chemical interaction of carboxyl groups with calcium ions also caused the self-organization described as the section of discussion.

Figure 3 shows the SEM images of HAp and HAp/ChS microparticles prepared by the spray drying method. The morphology of the microparticles was clearly different. The HAp microparticle had irregular shaped particles, doughnut and hollow particles. On the other hand, the HAp/ChS microparticles had perfectly spherical shape with the size range of 1-10μm. The microparticles had the size distributions of 1-20μm measured by laser diffraction method, which was almost same as the SEM observations. The mean particle size was ca 6μm.

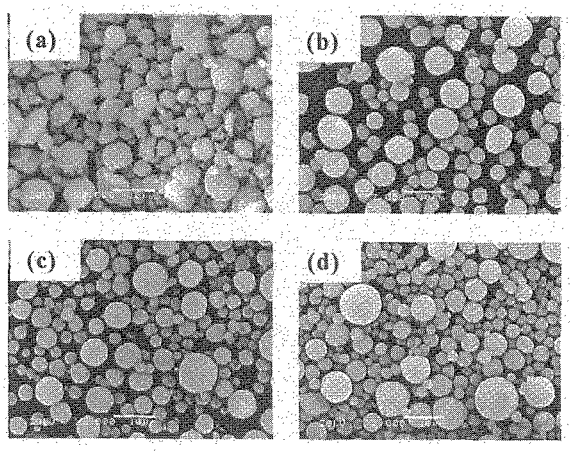


Fig. 3 SEM images of HAp and HAp/ChS microparticles obtained. (a) HAp, (b) 0.5 mg/ml, (c) 1.25 mg/ml and (d) 2.5 mg/ml of ChS concentrations.

TG-DTA analyses indicated that the ChS contents in the HAp/ChS microparticles obtained was almost same as the starting compositions. The exothermic peaks assigned to the ChS thermal decompositions were observed at 300°C. The weight ratio of HAp/ChS was calculated from the weight loss from the temperature range of 200 to 600 °C. The weight ratios of ChS/HAp were 3, 6 and 10 wt% for the starting concentrations of ChS as 0.5, 1.25 and 2.5 mg/l, respectively.

The specific surface area of HAp microparticle measured by BET method was 87.8$m^2$/g with the porosity of 58% which was calculated from the theoretical density (3.16g/$m^3$) of HAp. The increase of ChS contents (3, 6 and 10wt% in ChS/HAp weight ratio) in the HAp/ChS microparticles increased the surface area of 90.6, 114.6 and 115.7 $m^2$/g with the porosities of 64.6, 70.6 and 66.7%, respectively. The specific surface area was depended on the constituent crystal sizes. The surface area of microparticles obtained increased with the increase of the ChS contents. This tendency was almost matched with the decrease of crystallite size of HAp.

The zeta potential of HAp microparticles in the electrolyte solution was +3.5±1.6 mV. The increase of the ChS contents (3, 6, 10 wt%) in the microparticles decreased the zeta potentials of -16.2±2.8, -27.4±0.9 and -28.4 ±1.2 mV, respectively. The zeta potential of the microparticles containing over 10 wt% of ChS was almost constant at -28 mV. This indicated that the surface of microparticles was completely covered with ChS molecules.

## 4. DISCUSSION

The self-organization process is discussed as follows. The carboxyl and sulfate groups on ChS were ionized to charge negatively, to which calcium ions bound with strong ionic and/or weak covalent force. When a phosphate solution was dropped into the suspension, the nucleation of HAp occurred preferentially on the calcium ions bound to carboxyl groups and/or sulfate groups, and then the epitaxial growth of HAp nanocrystals occurred along the ChS molecular chains. It is considered that the 3/2 length of the HAp *c*-axis parameter (0.688 nm) was coincident with that of the adjacent 2 carboxyl and/or sulfate groups on ChS chains (1.02 nm). On the other hand, at the higher concentration of 2.5 mg/ml, the spindle-shaped aggregations were not observed as shown in Fig. 1 (c) and (d). It is concluded that the electrostatic repulsions among free functional groups of ChS with high negative charges repress the self-organization.

The crystal growth of HAp was inhibited at the initial concentrations of ChS in the $Ca(OH)_2$ suspensions over 2.5 mg/l. It is suggested that the $SO_3$ groups on the ChS molecule could inhibit the crystal growth of HAp.

The perfectly spherical microparticles of HAp/ChS nanocomposites were prepared by the spray drying method. M.C. Sunny et al. have also described the perfectly spherical microparticle of HAp prepared by S/W/O emulsion method [12]. The spray drying method has a benefit to obtain a large quantity of HAp and/or HAp/biopolymers microparticles at a time. The droplets in an atomizing process of the spray drying method are very stable because the suspensions of HAp/ChS nanocomposites had a higher viscosity compared with distilled water.

## 4. Conclusions

Three dimensionally organized nanocomposites of HAp and ChS with 150 × 50 nm in size were obtained through self-organization process under the lower ChS concentration of 2.5 mg/ml mixed into a $Ca(OH)_2$ suspension. The addition of ChS at higher concentrations inhibited the HAp crystal growth (maximum 32%) and also the self-organization. The perfectly spherical particles were successfully prepared by a spray drying method and the microparticles had the higher specific surface area than that of HAp. The microparticles of HAp/ChS nanocomposites will be applicable to create a substance of complicated more composites with a hierarchical structure and/or drug careers of therapeutic agents for the delivery system and the time controlled release.

## Reference

[1] H. Muir and T.E. Hardingham, "Structure of Proteoglycans", in *Biochemistry of Carbohydrates*, Vol. 5. ed. By W.J. Whelan. Butterworth / University Park Press, Baltimore, MD (1975), pp. 153.
[2] G.K. Hunter, S.K. Azigety, *Matrix*, **12**, 362 (1992).
[3] S.G. Rees, R.P. Shellis, G. Embery, *Biochem. Biophys. Res. Comm.*, **292**, 727 (2002).
[4] S. Shimabayashi, K. Itoi, *Chem. Pharm. Bull.*, **37(6)**, 1437 (1989).
[5] A.L. Boskey, L. Spevak, S.B. Doty, L. Rosenberg, *Calcif. Tissue Int.*, **61**, 298 (1997)
[6] S.G. Rees, D.T.H. Wassell, G. Embery, *Biomaterials*, **23**, 481 (2002).
[7] P. Luo and T.G. Nieh, *Biomaterials*, **17**, 1959 (1995).
[8] N. Patel, I.R. Gibson, S. Ke, S.M. Best, W. Bonfield, *J. Mater. Sci.: Mater. Med.*, **12**, 181 (2001).
[8] L.J. Cummings, T. Ogawa, P. Tunon, *Bio-Rad Bull.*, 1927 US/EG REV. A (1995).
[9] X. Zhang, J. Chen, X. Zhou, *Clin. Mater.*, 4, 319 (1989).
[10] M. Fabbri, G.C. Celotti, A. Ravaglioli, *Biomaterials*, **15**, 474 (1994).
[11] D.M. Liu, Biomaterials, **17**, 1955 (1996).
[12] M.C. Sunny, P. Ramesh and H.K. Varma, *Biomaterials*, **13**, 623 (2002)
[13] M. Itokazu, T. Sugiyama, T. Ohno, E. Wada, Y. Katagiri, *J. Biomed. Mater. Res.*, **39**, 536 (1998).
[14] H. Gautier, J. Guicheux, G. Grimandi, A.F. Chauvet, G. Daculsi, C. Merle, *J. Biomed. Mater. Res.*, **40**, 606 (1998).

(Received November 30, 2003; Accepted February 29, 2004)